

# Seismic Response Analysis of Base Isolated RC Building Considering Dynamical Interaction Between Soil and Structure



**T. Enomoto & T. Yamamoto**

*Kanagawa University, Yokohama, Japan*

**M. Ninomiya & Y. Miyamoto**

*Kozo Keikaku Engineering Inc., Tokyo, Japan*

**M. Navarro**

*University of Almeria, Almeria, Spain*

## SUMMARY:

The recently built RC building in campus of Kanagawa University in March, 2001 has L shaped plan with eight ground floors, two penthouse floors and two basement floors. This building has been installed base isolation system constituted by three type devices which are multi-layered elastomeric isolator, steel rod damper and lead damper. Inside and outside of this RC building, 7 seismometers with three components were installed. The strong motion observation was started from April, 2001 and about 100 earthquake strong motions were recorded by this vertical array observation system up to March, 2010 during 10 years. In this paper, we would like to present the results of dynamic response simulation of base isolated RC building using the revised SR Model considering dynamic interaction impedance around the building foundation.

*Keywords: Base Isolated RC Building, Soil-Structure Interaction System, Sway-Rocking Model*

## 1. INTRODUCTION

In general, the earthquake response of buildings is strongly influenced by surface soil structure (Navarro M. et al. 2007) and it's very important to consider the soil-structure interaction phenomena. The recently built RC building in campus of Kanagawa University in March, 2001 has L shaped plan with eight ground floors, two penthouse floors and two basement floors. This building has been installed base isolation system constituted by three type devices which are multi-layered elastomeric isolator, steel rod damper and lead damper (Enomoto et al. 2004). According to the structural design, the natural period of building in the fundamental mode was estimated about 0.79 sec without base isolated system and also about 1.4 sec with three type devices in the longitudinal direction (Uchiyama et al. 2001, Hikita et al. 2001, Adachi et al. 2001). Inside and outside of this RC building, 7 seismometers (5 seismometers were installed in building, 2 seismometers were installed in soil) with three components were installed. The strong motion observation was started from April, 2001 and about 100 earthquake strong motions were recorded by this vertical array observation system up to March, 2010 during 10 years (Enomoto et al. 2011). We analyzed the observed strong motions in order to investigate the dynamical response characteristics and also performed the dynamical response simulation using 2D dynamical interactions simulation by using Flush Program. The analytical results were good agreement with observed records at upper floors of base isolated floor but it's not good agreement with the lower floor of base isolated floor. In this paper, we would like to present the results of dynamic response simulation of base isolated RC building using the revised SR Model considering dynamic interaction impedance around the building foundation (Watanabe et al. 2009, Ninomiya et al. 2009). As the structural characteristics of objective base isolated building, the superstructure and basement structural were constructed by reinforced concrete and the base isolation system constituted by multi layered elastometric isolator, steel rod damper and lead damper, was installed between the superstructure and basement structure. This building has two basement floors, eight ground floors and two floors of penthouse on the top of building. The strong motion observation system was installed in the building and surrounding soils. Five accelerometers were installed in different floors, B2F, B1F, 3F, 5F and 8F and two accelerometers were located at surface and basement level of surrounding soil. The earthquake response analysis model considering dynamic interaction impedance around the

foundation is SR, sway-rocking, model that was modelled by the interaction spring and damping calculated by 3 dimensional thin layered element method (Damping Committee of AIJ 2004, Interaction Committee of AIJ 2002, Interaction Committee of AIJ 2005).

We have examined the results of comparison between the observed seismic motions and the dynamical response simulated results at 2nd basement floor level located just below of seismic isolation layer, and also we compared the 1st basement floor level and 3rd, 6th, 8th floor level above the ground. As the results, the comparison of results between observed and dynamical response analysis by using SR model considered dynamical impedance around building foundation at 2nd basement floor level appeared well agreement each other.

**2. OBJECT OF THIS RESEARCH**

At Kanagawa University’s Building No. 23 (base-isolated RC building), seismic observations are carried out in the ground and the building. Diagrams of restoring force loops according to amplitude level were prepared using relative story displacement - story shear force of the base isolation layer calculated from observation records of earthquakes recorded up to now with relatively large observation record values, and the dynamic characteristics of the base isolation layer were examined. Also, an analysis model incorporating the results was prepared and a dynamic analysis using a finite element analysis program was conducted. Then, a comparison/examination of the dynamic analysis results and seismic response characteristics based on the observation records was carried out. As a result, inconsistencies were found mainly in the response analysis results for the base isolation layer, and these are considered to be due to the effect of dynamic interaction between the ground and the building. The objective of this research is to consider the effect of interaction on behavioural characteristics of a base-isolated building by accurately calculating interaction impedance of the ground around the foundation, and to re-examine dynamic behaviour in the subject building by conducting a simulation that incorporates a base isolation layer elastic-plastic analysis method.

**3. OVERVIEW OF BUILDING AND PREVIOUS ANALYSIS MODELS**

**3.1. Overview of building**

Building No. 23 is an RC framed structure with 2 floors below ground, 8 floors above ground, and a rooftop structure containing 2 floors. The building is an intermediate base-isolated structure with a base isolation layer between the 1st and 2nd below-ground floors. Figure 1 shows an elevation view of the subject building. The installed seismometers are servo accelerometers and they are installed on 5 floors (8F, 6F, 3F, B1F, and B2F) in roughly the same position on each floor. Vertical array observations are carried out at 2 locations; at the ground surface (GL -1.5 m) and underground (GL -21.8 m) approximately 30 m from the building.

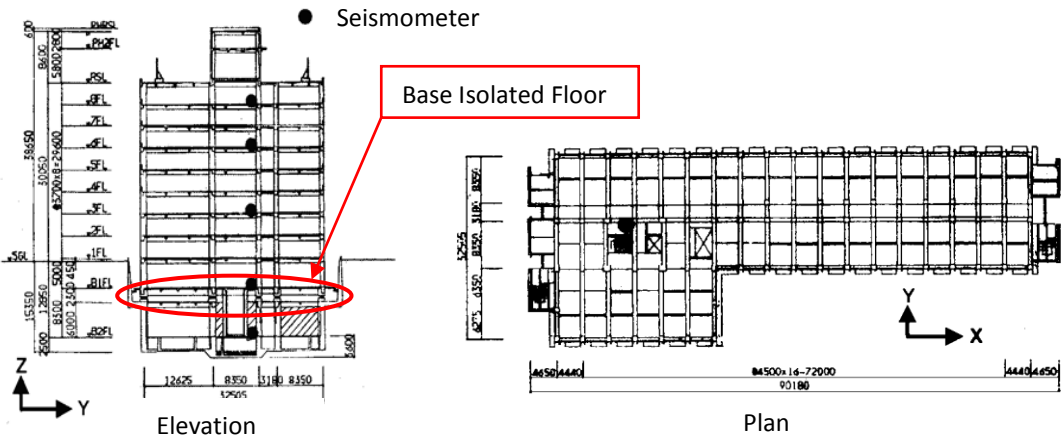
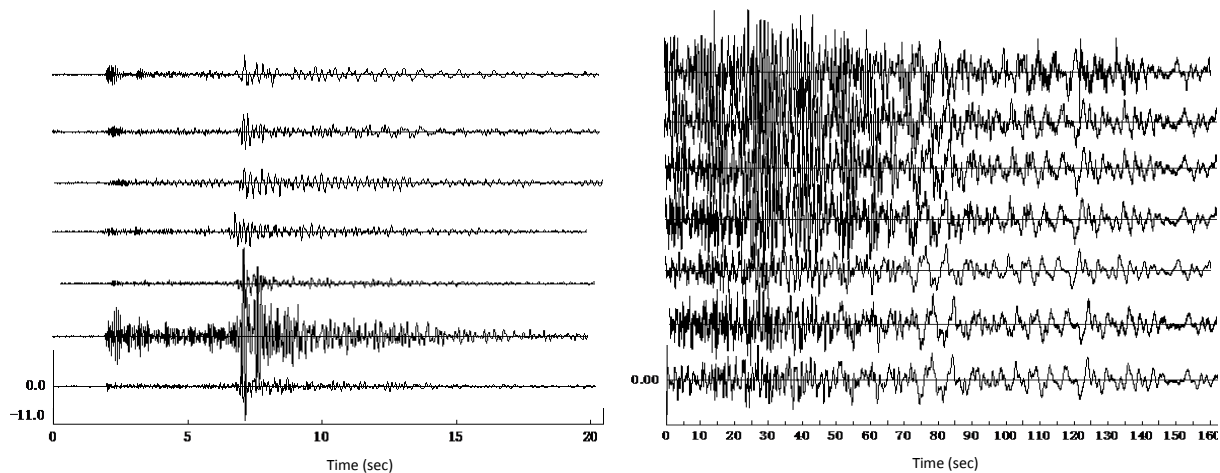


Figure 1 Elevation and plan view of No.23 building

### 3.2. Observation records

The observed waveforms are arranged into X (NS component), Y (EW component), and Z (vertical component) for each floor using acceleration records obtained from the seismometers installed in 7 locations; underground (GL -21.8 m) and at the ground surface (GL -1.5 m) near Building No. 23, B1F, B2F, 3F, 6F, 8F). The examples of observed acceleration records are indicated in Figure 1. In this research, large-, medium-, and small-scale seismic motions were selected from the observation records that have been recorded so far. Specifically, an earthquake on July 23, 2005 was taken as a large earthquake indicated (a) in Table 1, an earthquake on May 19, 2002 was taken as a medium earthquake indicated (b) in Table 1, and an earthquake on June 20, 2006 was taken as a small earthquake indicated (c) in Table 1, and a surface response analysis was carried out using these seismic observation records.



(1) Short Distance Eq. (30<sup>th</sup> Jan. 2009)

(2) Long Distance Eq. (14<sup>th</sup> Jun, 2008)

Figure 1 Example of Observed Records (From up to down, 8F, 6F, 3F, B1F, B2F, GL-1.5m, GL-21.8m)

Table 1 Seismic observation record

	Origin Time	Location of Epicenter	Magnitude	Maximum Acc. at Ground Surface		
				X-Dire.(gal)	Y-Dire.(gal)	Z-Dire.(gal)
(a)	23rd July, 2005	NW Part of Chiba Pref.	6.0	147.0	141.0	57.6
(b)	19th May, 2002	NW Part of Chiba Pref.	4.6	16.1	49.3	15.9
(c)	20th June, 2006	NW Part of Chiba Pref.	6.0	11.1	14.1	4.5

### 3.3. Restoring force characteristics of base isolation layer for observed waves

In order to examine the dynamic characteristics of the base isolation layer from the observed strong motion records, the story shear force ( $Q$ ) at the base isolation layer was calculated using Equation (3.1) by consolidating the building taking into account the installation positions of the seismometers, as in Figure 3. Also, the relative story displacement ( $\delta$ ) of the base isolation layer was found by integrating the observation records for B1F and B2F, the floors above and below the base isolation layer, using Equation (3.2).

From these, hysteresis loops for the base isolation layer were drawn and equivalent shear stiffness ( $k_e$ ) was calculated.

$$Q_{B2F(t)} = \sum_{i=B1F}^{RF} \frac{W_i}{g} \ddot{X}_i(t) \quad (3.1)$$

$$\delta(t) = \delta_{B1F}(t) - \delta_{B2F}(t) \quad (3.2)$$

Where,

$Q_{B2F(t)}$  : Story shear force acting on base isolation layer

$W_i$  : Weight of story i

$g$  : Acceleration of gravity

$\ddot{X}_i(t)$  : Horizontal response acceleration of story i

$\delta(t)$  : Relative displacement between floors above/below base isolation layer

$\delta_{B1F}(t)$  : Absolute displacement of horizontal response of B1F

$\delta_{B2F}(t)$  : Absolute displacement of horizontal response of B2F

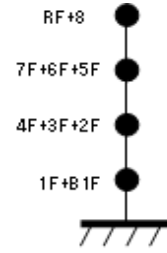


Figure 3 Schematic multiple mass-spring model for No.23 building

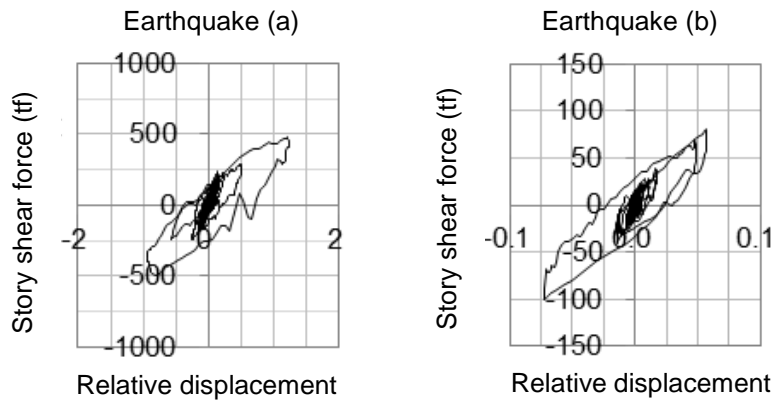


Figure 4 Hysteresis loops for base isolation layer for observed waves

### 3.4. Previous analysis results

Although analysis results and observational results were largely in agreement at each floor above the base isolation layer, discrepancies were clearly found at the basement floor located below the base isolation layer. A comparison with the acceleration Fourier spectra of Earthquake at B2F and 8F is shown in Figure 5. Reasons for these discrepancies include the fact that dynamic interaction between the ground and the building is not fully taken into account in the analysis model. Also, because the core of the analysis assumes the building is in an elastic state and the shear stiffness of the base isolation layer is set as an equivalent stiffness based on vibration amplitude level, it is difficult to say that the analysis model accurately evaluates the behaviour of a base-isolated building considering that stiffness depends on vibration amplitude during the earthquake and changes from minute to minute.

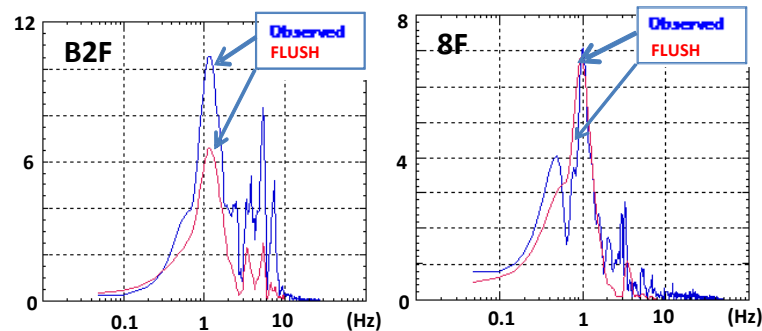


Figure 5 Acceleration Fourier spectra comparison diagram

## 4. ESTABLISHING THE ANALYSIS MODEL TABLES

### 4.1. Modeling of building

When preparing the analysis model in this research, in order to carry out the intended analysis that considers dynamic interaction, mass distribution and stiffness distribution were re-examined. Using a structural calculation program, the quantity of columns, beams, slabs, walls, etc. in the building were inputted/arranged, and the loading on each story was calculated by inputting fixed loads as well as loads on floors according to the purpose of each room (live loads). The rest of the analysis was done using data converted from the outputted 3D model to a multi-mass model.

### 4.2. Incremental loading analysis

It was decided to evaluate stiffness from period and story drift angle by carrying out an incremental loading analysis of the multi-mass model. The analysis used RESP-F3, which is capable of finding restoring force characteristics of each member from inputted cross-sections, reinforcement arrangements, etc. and carrying out 3D elastic-plastic analysis using the load incremental method, and RESP-QDM, which is capable of preparing skeleton curves with multiple polylines from story shear force and relative story displacement obtained from the results of this incremental loading analysis and converting them into vibration analysis data.

### 4.3. Modelling of base isolation layer

In order to incorporate the base isolation layer into the building model, the restoring force characteristics of base isolation members are inputted. Steel rod dampers were inputted as bilinear, lead dampers as completely bilinear, and laminated rubber as elastic (because the natural rubber used is elastic and does not absorb energy).

### 4.4. Evaluation of interaction spring using impedance analysis

The impedance analysis is carried out by modelling the foundation and the ground around the foundation and using an analysis program that combines a 3D finite element method and the thin-layer element method. The impedance of the ground around the foundation is calculated assuming the Sway-Rocking model (hereafter, SR model) shown in Figure 6. Equation (4.1) is the equation of motion at the center of gravity of the foundation, taking into account interaction.

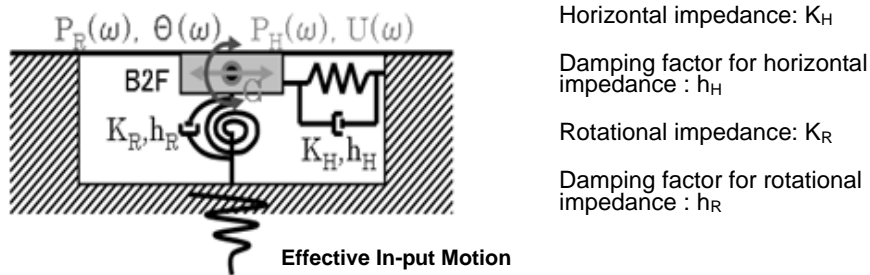


Figure 6 SR model considered the interaction impedance between soil and foundation

$$\left( -\omega^2 \begin{bmatrix} M & 0 \\ 0 & J \end{bmatrix} + \begin{bmatrix} K_{HH}(\omega) & K_{HR}(\omega) \\ K_{HR}(\omega) & K_{RR}(\omega) \end{bmatrix} \right) \begin{Bmatrix} U(\omega) \\ \Theta(\omega) \end{Bmatrix} = \begin{Bmatrix} P_H(\omega) \\ P_R(\omega) \end{Bmatrix} \quad (4.1)$$

Where,

$K_{HH}$ : Horizontal impedance

$K_{RR}$ : Rotational impedance

$K_{HR}$ : Horizontal-rotational coupled impedance

$M$  : Foundation weight,  $J$ : Moment of inertia  
 $U(\omega)$ : Foundation horizontal motion,  
 $\Theta(\omega)$ : Foundation rotational motion  
 $P_H(\omega)$ : Horizontal excitation force,  
 $P_R(\omega)$ : Rotational excitation force

The calculated impedance is shown in Figure 7. Ground spring constants in the SR model use real part values. Also, the gradient of the imaginary part represents the damping factor; however, it was converted to the damping factor commonly used in building design using Equation (4.2) and the results are shown in Figure 8.

$$\begin{aligned}
 h_H &= \sin(0.5(\tan^{-1}(\text{Im}(K_{HH}) / \text{Re}(K_{HH})))) \\
 h_R &= \sin(0.5(\tan^{-1}(\text{Im}(K_{RR}) / \text{Re}(K_{RR}))))
 \end{aligned}
 \tag{4.2}$$

Where,

$h$ : Damping factor  
 $\text{Re}(K)$ : Impedance real part  
 $\text{Im}(K)$ : Impedance imaginary part  
 Subscript H indicates horizontal direction, subscript R indicates rotational direction

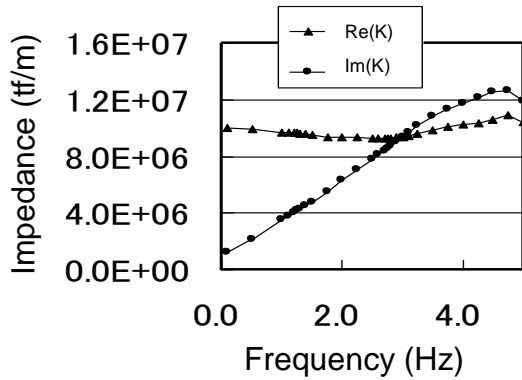


Figure 7 Horizontal impedance ( $K_{HH}$ )

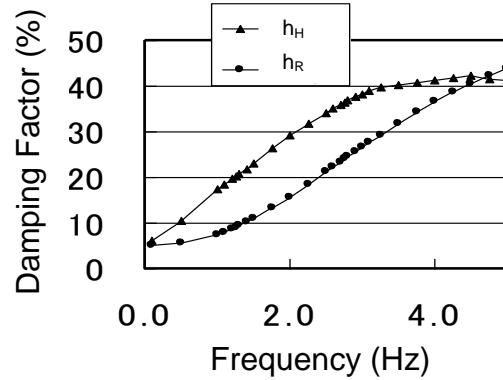


Figure 8 Equivalent viscous damping factor

#### 4.5. Preparation of Whole-System SR Model

From these results, a whole-system SR model was prepared, as in Figure 9, by combining the SR model that takes into account the equation of motion in Equation (3) and equivalent foundation interaction with an elastic-plastic seismic response analysis program prepared through building modeling incorporating the restoring force characteristics of the base isolation layer, and dynamic behaviour of the base-isolated building was examined.

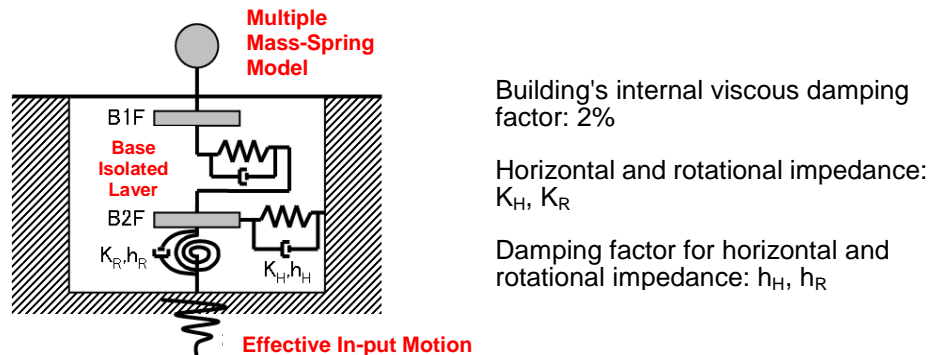


Figure 9 Conceptual Modeling by SR model (whole system) for No.23 Building

**5. Elastic-Plastic Seismic Response Analysis**

Using the above-mentioned SR model, an elastic-plastic analysis is carried out using a building structure vibration analysis program (RESP-M/II, Kozo Keikaku Engineering Inc.). Acceleration, acceleration Fourier spectra, and base isolation layer hysteresis loops are calculated for the three Earthquakes (a), (b), and (c) outlined in Section 2-2, which are the analysis waves for comparison. The restoring force characteristics of the base isolation layer are changed and the analysis is carried out in two patterns; Analysis 1 and 2. Details are given below. Diagrams comparing the analysis results for Analysis 1 and 2 with the observed wave for each earthquake are shown for acceleration waveforms (Figures 10, 13, 16), acceleration Fourier spectra (Figures 11, 14, 17), and base isolation layer hysteresis loops (Figures 12, 15, 18).

**Analysis 1 :**

Base isolation layer is replicated by inputting stiffness of base isolation members of the relevant building using the program’s existing restoring force characteristics. Restoring force characteristics for each base isolation member are inputted/outputted. These results are calculated and included in analysis program (RESP-M/II) as the restoring force loops for base isolation members and calculated result is shown in Figures 12, 15, and 18.

**Analysis 2 :**

It is evident that both acceleration response and period resulting from Analysis 1 are outputted relatively large. Therefore, considering there to be a discrepancy in the damper performance evaluation of base isolation members, restoring force characteristics of the base isolation layer were corrected based on observation records. Correction was carried out focusing on initial stiffness values on the hysteresis loop.

The comparisons between observed wave and calculated wave used above mentioned SR model on 3 types earthquakes are summarized as follows. In case of large-scale earthquake as indicated (a) in Table 1, wave forms, Fourier spectra and restoring force characteristics (hysteresis loops) at base isolated layer are shown in Figure 10, 11, 12. Also, in case of medium-scale earthquake as indicated (b), wave forms, Fourier spectra and restoring force characteristics at base isolated layer are shown in Figure 13, 14, 15. And finally, in case of small-scale earthquake as indicated (c), wave forms, Fourier spectra and restoring force characteristics at base isolated layer are shown in Figure 16, 17, 18.

1) Analytical result for earthquake (a), large-scale earthquake

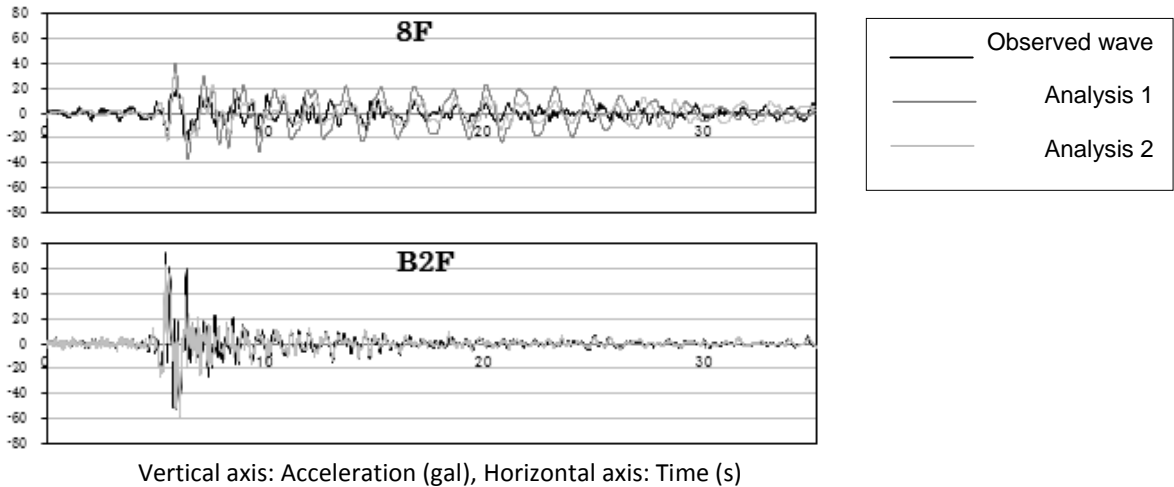
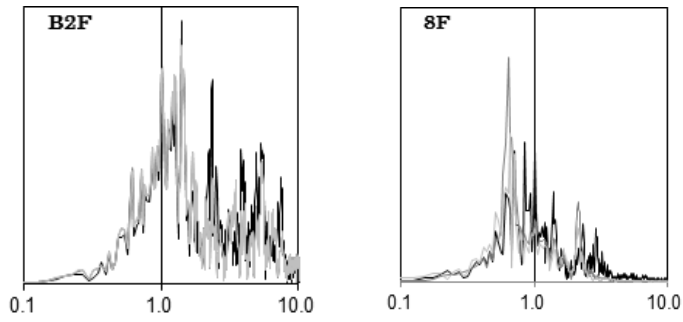


Figure 10 Acceleration waveforms during Earthquake (a)



Vertical axis: Fourier Spectral Amplitude (gal\*sec),  
Horizontal axis: Frequency (Hz)

Figure 11 Acceleration Fourier spectra during Earthquake (a)

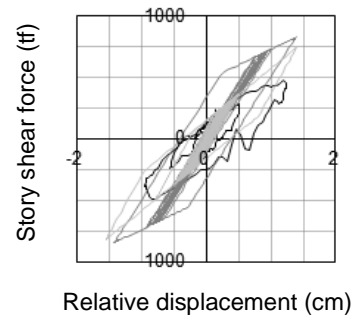
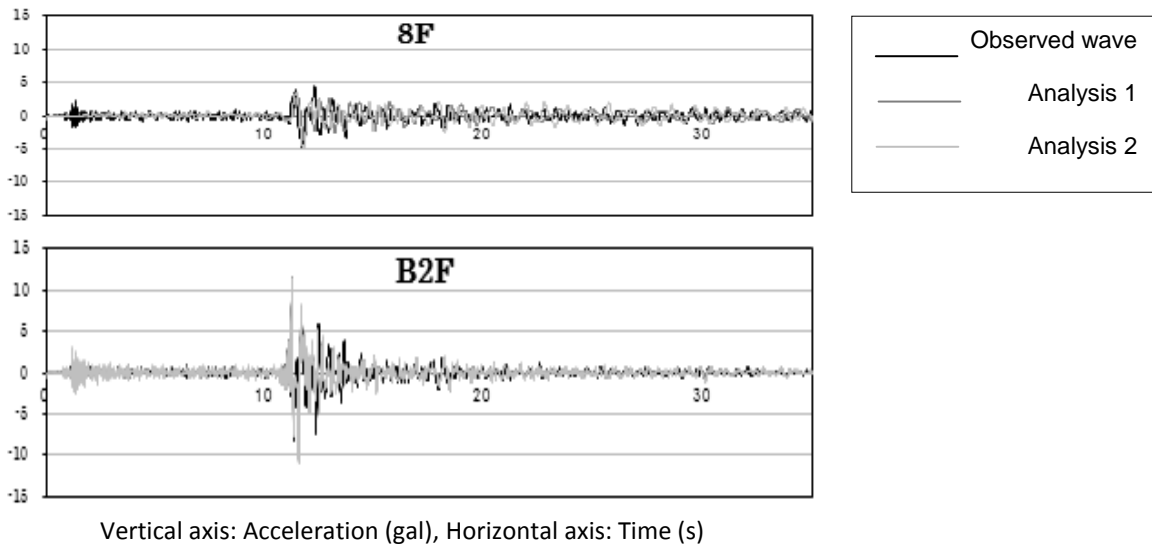


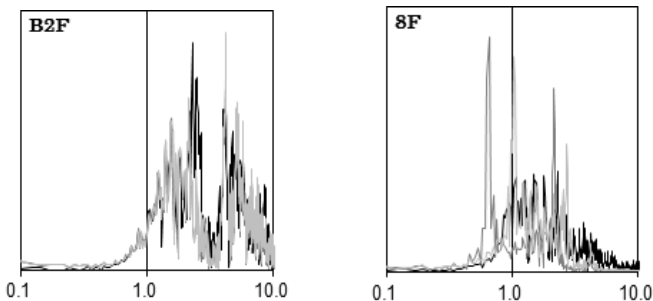
Figure 12 Restoring force loops for base isolation layer during Earthquake (a)

2) Analytical result for Earthquake (b), medium-scale earthquake



Vertical axis: Acceleration (gal), Horizontal axis: Time (s)

Figure 13 Acceleration waveforms during Earthquake (b)



Vertical axis: Fourier Spectral Amplitude (gal\*sec),  
Horizontal axis: Frequency (Hz)

Figure 14 Acceleration Fourier spectra during Earthquake (b)

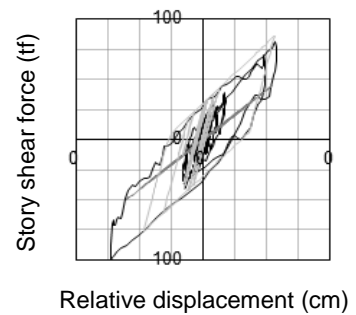


Figure 15 Restoring force loops for base isolation layer during Earthquake (b)

3) Analytical result during Earthquake (c), small-scale earthquake

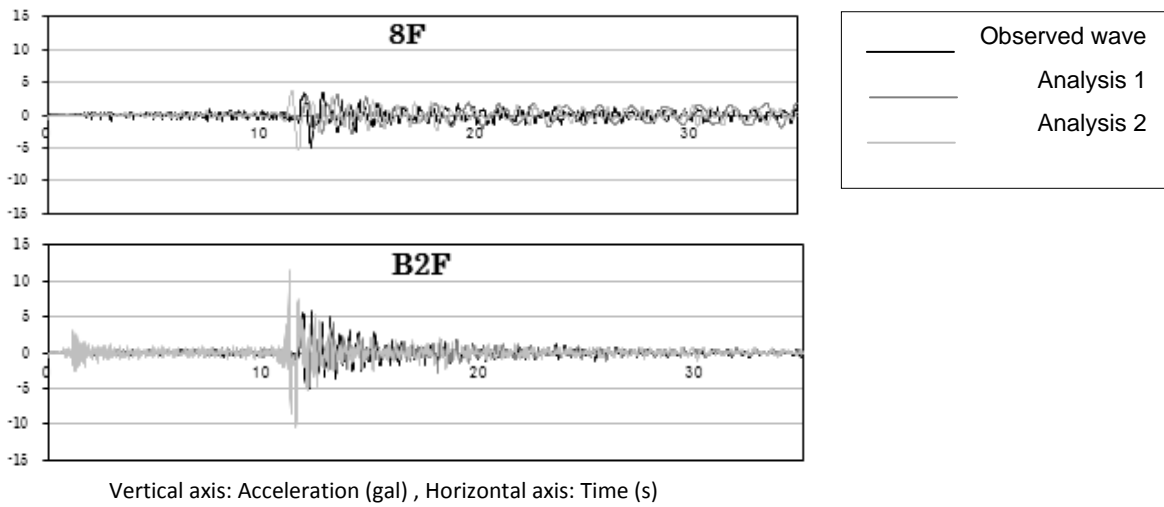


Figure 16 Acceleration waveforms during Earthquake (c)

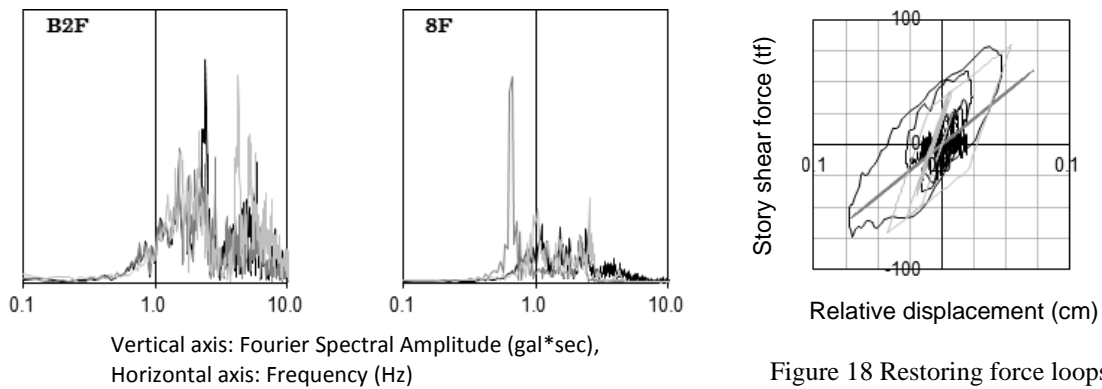


Figure 17 Acceleration Fourier spectra during Earthquake (c)

Figure 18 Restoring force loops for base isolation layer during Earthquake (c)

## 6. ANALYSIS RESULTS

It was confirmed that, by introducing the SR model, the response on B2F during earthquakes of different sizes is represented in a way that is consistent with the observational results. This showed that input of impedance is appropriate and the effect of interaction plays a role in response. However, as we move up the building, the acceleration response increases, and it is evident from the impedance diagrams that period also increases (Analysis 1). This effect is considered to be due to the restoring force characteristics of the base isolation members, considering the difference between the base isolation layer hysteresis loops and the observed wave, and when the restoring force characteristics were corrected to make the hysteresis loops take more account of information obtained from observational results and inputted, both response values and period improved.

## 7. CONCLUSION

This research analysed seismic response in a base-isolated building by preparing a SR model using interaction impedance for interaction between the ground and the building, and examining restoring force characteristics for the base isolation layer. In this way, the model was improved so that response values largely agreed with observed values on B2F, the building's lowest floor. Also, the validity of

modelling the restoring force characteristics of the base isolation layer with steel rod dampers in an elastic state was confirmed. In regard to earthquakes of a larger scale than those examined here, an earthquake in which both dampers are plasticized has not yet been observed, and because there is believed to be a high probability that the ground also becomes plastic prior to plasticization of steel rod dampers, review including impedance is necessary. Therefore, an accurate evaluation of restoring force characteristics during a large-scale earthquake is not possible at this time. Stiffness of base-isolated buildings changes from moment to moment during an earthquake due to drift. In this research as well, attempts were made to examine constantly changing stiffness in the SR model, but hardly any change could be seen at the level of Earthquake. Hereafter, we intend to study behavioural characteristics during a large-scale earthquake in which the relative story displacement of the base isolation layer exceeds the yield point of the steel rod dampers.

#### **ACKNOWLEDGEMENTS**

This research was supported by TEDCOM (Typhoon and Earthquake Disaster Control Management) Research Project conducted by Kanagawa University from 2000 to 2005 funded by the Japanese Ministry of Education, Science, Sports and Culture. And we would like to express the great gratitude to all those who participate the analysis of strong motion records by Kanagawa University's dynamic behaviour observation system, especially, Yuya Watanabe who was a student of graduated school of Kanagawa University and contributed to establish the model used in this research.

#### **REFERENCES**

- Adachi N. et al. (2001), Vibration Tests for Building No. 23 (base isolated) and New Building No. 1 at Kanagawa University: Part 3, Annual Meeting Architectural Institute of Japan
- Damping Committee of AIJ(2004), Damping in Buildings, Architectural Institute (AIJ) of Japan
- Enomoto T., Kuriyama T., Yamamoto T., Navarro M. (2002), Dynamic Behaviour of Base-isolated RC Building, Eurodyn2002, 5th International Conference on Structural Dynamics, CD-ROM, Munich, Germany, Aug.
- Enomoto T., Ninomiya M., Navarro M. (2011), Comparison of Seismic Response Characteristics Between Non Base-isolated and Base-isolated Building, Eurodyn2011, 8th International Conference on Structural Dynamics, CD-ROM, Leuven, Belgium, July
- Hikita T. et al(2001)., Vibration Tests for Building No. 23 (base isolated) and New Building No. 1 at Kanagawa University: Part 2, Annual Meeting Architectural Institute of Japan
- Interaction Committee of AIJ(2002), An Introduction to Dynamic Soil-Structure Interaction, Architectural Institute (AIJ) of Japan
- Interaction Committee of AIJ(2005), Seismic Response Analysis and Design of Buildings Considering Dynamic Soil-Structure Interaction, Architectural Institute (AIJ) of Japan
- Navarro, M., Vidal, F., Enomoto, T., Alcalá, F.J., Sánchez, F.J. and Abeki, N. (2007). Analysis of site effects weightiness on RC building seismic response. The Adra (SE Spain) example. Earthquake Engineering and Structural Dynamics, 36, 1363-1383.
- Ninomiya M. et al. (2009), Seismic Response Analysis of Base-Isolated RC Buildings Considering Dynamic Interaction Impedance of Surrounding Soil (Part 2), Annual Meeting Architectural Institute of Japan, Aug.
- Uchiyama H. et al.(2001), Vibration Tests for Building No. 23 (base isolated) and New Building No. 1 at Kanagawa University: Part 1, Annual Meeting Architectural Institute of Japan
- Watanabe Y. et al. (2009), Seismic Response Analysis of Base-Isolated RC Buildings Considering Dynamic Interaction Impedance of Surrounding Soil (Part 1), Annual Meeting Architectural Institute of Japan, Aug.